PARALLEL-HOLE COLLIMATOR DESIGN

We wish to bring to your attention an error which has appeared in the literature on parallel-hole multichannel collimator design and optimization. Our studies have shown the geometric resolution equation as given by Anger (*1*) and used by others (*2,3*) to be in error.

For a collimator fixed in position, the gamma-ray distribution has the irregular shape shown in Fig. 1 (*1*). If the collimator is assumed to move during exposure, the gamma-ray distribution becomes the smoothed triangular pattern shown. The geometric resolution, R, is defined as the full width at half the maximum value of this smoothed intensity distribution curve. The equation defining R is derived from geometric considerations. Referring to Fig. 1, the triangle ΔLMN is congruent to the triangle ΔEFG; therefore, the geometric resolution is

$$R = \frac{D}{A_E}(A + B + C), \qquad (1a)$$

where $A_E = A - 2/\mu(E)$ is the effective collimator thickness. This resolution equation differs from that given by Anger (*1*) and used by others (*2,3*) where

$$R_A = \frac{D}{A_E}(A_E + B + C). \qquad (1b)$$

When B + C is assumed equal to zero the resolution from Eq. (1b) is $R_A = D$. This result indicates that no septal penetration occurs. The resolution given

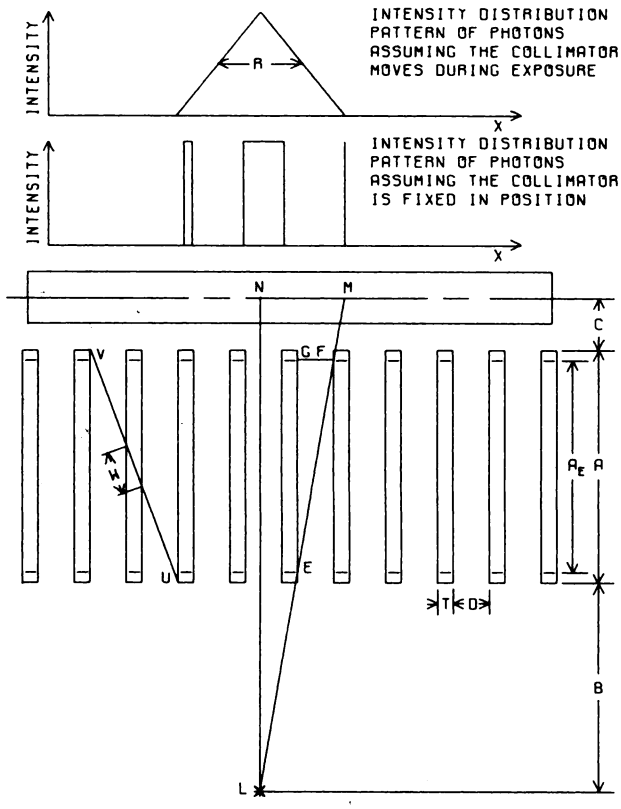

FIG. 1. Cross section of parallel-channel collimator showing gamma-ray pathways and irradiated areas of detector.

TABLE 1. OPTIMIZED COLLIMATOR GEOMETRIC PARAMETERS* AND COMPARISON OF THE PREVIOUSLY APPLIED RESOLUTION EQUATION AND THE CORRECTED RESOLUTION EQUATION†

Collimator number	1			2			3			4		
Nominal maximum photon energy (keV)	200			280			360			410		
Hole length, A (mm)	25.4			38.1			55.9			66.0		
Hole diameter, D (mm)	2.82			3.81			4.9			5.4		
Septum thickness, T (mm)	0.77			1.52			2.26			2.70		
Gamma-ray energy (keV)	140			280			360			410		
Geometric efficiency ($\times 10^{-4}$)	4.60			6.77			3.01			1.73		
Geometric resolutions (mm)	R_A	R	$\frac{R-R_A}{R_A}$(%)	R_A	R	$\frac{R-R_A}{R_A}$(%)	R_A	R	$\frac{R-R_A}{R_A}$(%)	R_A	R	$\frac{R-R_A}{R_A}$(%)
B = 25.4 mm	5.78	5.87	1.56	6.71	7.16	6.70	7.47	8.11	8.60	7.76	8.63	11.21
B = 76.2 mm	11.60	11.68	0.69	12.40	12.85	3.63	12.51	13.15	5.12	12.37	13.34	7.85
B = 127.0 mm	17.41	17.50	0.52	18.08	18.54	2.54	17.55	18.19	3.65	16.99	18.16	6.90

* Collimator geometric parameters are those used in Table IV of (1).
† All collimators are slab constructions fabricated from lead assuming a penetration factor of 0.05.

by Eq. (1a) for $B + C = 0$ is

$$R = \frac{DA}{A_E} \cong D\left(1 + \frac{2}{A\mu(E)}\right) \qquad (2)$$

which accounts for septal penetration at the edges of the collimator holes.

A comparison of the resolution calculated from each result is given in Table 1. (For a detailed explanation of the origin of the collimator parameters given in Table 1, see Ref. *1*.) It is seen that for a collimator designed for high-energy gamma rays (≧400 keV), the error in the resolution is 10% or greater for small source-to-collimator distances. This error is reduced for lower energy gamma and large source-to-collimator plus collimator-to-detector distances.

MARK S. GERBER
DON W. MILLER
Ohio State University
Columbus, Ohio

REFERENCES

1. ANGER HO: Radioisotope cameras. In *Instrumentation in Nuclear Medicine*, Hine GH, ed, New York, Academic Press, 1964, pp 485–552

2. KELLER EL: Optimum dimensions of parallel-hole, multi-aperture collimators for gamma-ray cameras. *J Nucl Med* 9: 233–235, 1968

3. WALKER WG: Design and analysis of scintillation camera lead collimators using a digital computer. In *Medical Radioisotope Scintigraphy*, vol 1, Vienna, IAEA, 1969, pp 545–560

FOCAL HYPERFIXATION OF RADIOCOLLOID BY THE LIVER

In recent years, several cases of focal hyperfixation of radiocolloid in the liver scan have been presented in the *Journal of Nuclear Medicine*. The reason for this hyperfixation could not be determined in most cases. We observed one with a "hot spot" in the liver scan which could be examined histologically.

A 37-year-old female patient consulted her physician for discomfort in the epigastrium. At physical examination there was a clearly delimited round and palpable mass. Blood chemistry revealed no pathologic findings except for a slight rise in alkaline phosphatase and SGOT. The patient was referred to us for a liver scan, which showed a hot spot, corresponding to the palpable tumor in the epigastrium. Angiographic examination was suggestive of a tumor in the liver (Fig. 1). Therefore, the patient was operated on and left lobectomy was carried out. The pathologist found a well-defined tumor with a diameter of 6 cm in the left lobe of the liver. Histologically, the tumor consisted of normal liver tissue with moderate fibrosis. Histologic diagnosis: hamartoma in the left lobe of the liver.

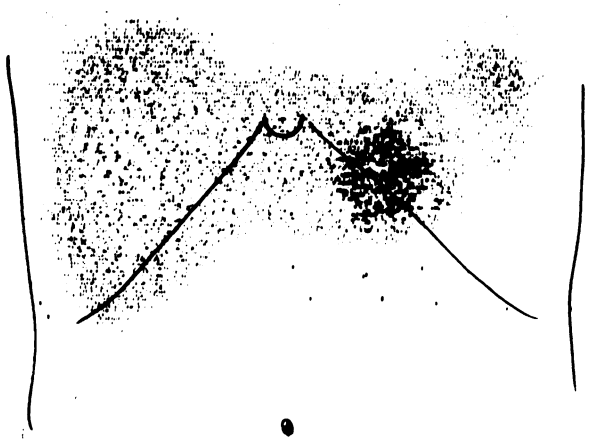

FIG. 1. Angiographic examination suggestive of liver tumor.

J. PASQUIER
Hôpital Cantonal
Fribourg, Switzerland

T. DORTA
Kantonsspital
Chur, Switzerland

EXPRESSION OF TISSUE ISOTOPE DISTRIBUTION

When tissue-distribution studies of labeled compounds are reported, the common method of expressing individual tissue concentration is as percent of administered dose per gram of tissue. To be meaningful, the size of the animal must be stated, since, obviously, a large animal will constitute a larger dis-